JOURNAL OF MATERIALS SCIENCE **40** (2005) 53–62

Epoxidised natural rubber/silica hybrid nanocomposites by sol-gel technique: Effect of reactants on the structure and the properties

A. BANDYOPADHYAY, M. DE SARKAR, A. K. BHOWMICK*
Rubber Technology Center, Indian Institute of Technology, Kharagpur-721302, India
E-mail: anilkb@rtc.iitkgp.ernet.in

This paper reports the effects of various reaction parameters such as solvent, mole ratio of water to tetraethoxysilane and temperature on the structure and the properties of epoxidised natural rubber/silica organic-inorganic hybrid nanocomposites, prepared by sol-gel technique. The sol-gel reaction was conducted at a constant concentration of tetraethoxysilane (45 wt% with respect to the rubber), used as the precursor for silica under a constant pH of 1.5. Infrared spectroscopic studies and the ash content data indicated the maximum silica generation in tetrahydrofuran compared to chloroform and carbon tetrachloride, which are less polar and had low affinity towards water than the former. The silica particles prepared from tetrahydrofuran were scattered within the rubber matrix with an average dimension of 100 nm, as evident from the transmission electron microscopic study. Dispersion of nanosilica within the composites was obtained when the tetraethoxysilane to water mole ratio was maintained up to 1:2, beyond which the resultant composites showed phase separation due to the agglomeration of the silica particles. High gelling temperature of the hybrids also resulted in phase separated morphology, probably due to the accelerated condensation reaction in the composites. All the phase separated composites showed higher infrared optical density and transmission loss compared to the nanocomposites. Poor mechanical reinforcement was observed from the dynamic mechanical analysis of the uncured composites having larger silica particles. On the contrary, better mechanical properties were achieved with the nanocomposites containing 90–100 nm silica. The nanocomposite prepared with 1:2 tetraethoxysilane to water mole ratio in tetrahydrofuran under room temperature showed the highest tensile strength and 100% tensile modulus, probably due to better polymer-filler interaction, in the uncrosslinked state and after crosslinking. *© 2005 Springer Science + Business Media, Inc.*

1. Introduction

One of the most popular ways to prepare organic-inorganic hybrid is the sol-gel chemistry [1–3]. The sol-gel process begins with a combination of metal alkoxide precursors $[M(OR)_n]$ and water, where M is a network forming element. Hydrolysis and condensation are the two fundamental steps to produce a network in the presence of an acidic catalyst. The entire reaction scheme can be presented through Scheme 1 [4].

$$\text{M-OR} + H_2O \underset{\text{Esterification}}{\overset{\text{Hydrolysis}}{\rightleftharpoons}} \text{M-OH} + \text{R-OH} \quad R = \text{alkyl group.}$$

$$\text{M-OH} + \text{HO-M} \underset{\text{Hydrolysis}}{\overset{\text{Water condensation}}{\Delta}} \text{M-O-M} + H_2O$$

Scheme 1

Water and alcohol are the by-products of the sol-gel reaction. Tetraethoxysilane is the most widely practiced metal alkoxide for the preparation of the polymer/silica hybrid composites, as it contains four hydrolysable groups. Interactions between the polar functional groups of the polymer and the residual silanol groups of the silica phase restricts micro-phase separation within the hybrid composites and facilitates nanolevel dispersion of the filler particles in polymer matrix [5].

The proportion of different chemicals mixed to prepare the sol plays a substantial role in fabricating a hybrid composite. Formulation of the sol governs the microstructure of the gel body. The parameters that influence the sol-gel reaction are the amount of organic and inorganic components, the mole ratio of H_2O/alkoxysilane, solvents, reaction temperature and

---

*Author to whom all correspondence should be addressed.

pH of the reaction medium. The present work is an investigation of these factors excluding the last one, which forms another communication. In our laboratory, rubber/clay nanocomposites using solution intercalation technique have been successfully prepared which show substantial improvements in mechanical properties over the control elastomers [6–8]. Nanosilica reinforcement of the polar polymers like acrylic rubber [9], poly (vinyl alcohol) [10] and epoxidised natural rubber [11] using sol-gel technique has also been reported recently by us.

Solvent is used to dissolve the polymer and the sol-gel reaction is carried out in the solution phase. The dielectric constant (ε) of the solvent plays an important role. The ε value demonstrates the polarity of the solvent. It has been found that by changing the polarity of the solvents, the rates of hydrolysis and condensation of the alkoxysilane are affected [12, 13]. The proportion of water to alkoxysilane ratio is also important, as water hydrolyses alkoxysilanes and can therefore influence the formation of silica within the composites. Temperature controls the rate of the chemical reaction. This paper reports the effects of variation of the nature of solvents, water to tetraethoxysilane mole ratio and the temperature for condensation reaction on the structure and properties of epoxidised natural rubber/silica organic-inorganic hybrid nanocomposites.

Epoxidised natural rubber with 50 mole percent of epoxy content is fairly polar in nature and could act as the matrix for the sol-gel reaction [11]. In our earlier communication we have reported the formation of a new type of organic-inorganic hybrid nanocomposites generated from epoxidised natural rubber and silica by using the above technique. Transparent hybrid composites have been obtained up to 50 wt% of tetraethoxysilane loading, which acts as the silica precursor in the hybrid. The rubber has been found to interact chemically with the filler at 40 and 50 wt% of tetraethoxysilane loading.

The pH of the reaction medium was kept constant to 1.5 by adding appropriate amount of concentrated HCl. The proportion of tetraethoxysilane was fixed to 45 wt% with respect to the rubber used.

2. Experimental

2.1. Materials

Epoxidised natural rubber (ENR50, with 50 mol% of epoxy content, Mooney viscosity $ML_{(1+4)}100^\circ C = 140$), was supplied by the Rubber Board, Kottayam, India. Henceforth, the rubber will be designated as only ENR. Tetraethoxysilane, (TEOS, density = 930 kg/m^3) was procured from ACROS Organics, USA. Dicumyl peroxide (DCP, 99% pure) was purchased from Aldrich Chemicals, USA. Deionized water and concentrated hydrochloric acid (laboratory grade) were obtained from indigenous sources. The solvents: tetrahydrofuran (THF), chloroform ($CHCl_3$) and carbon tetrachloride (CCl_4), employed for the current study were all of laboratory grade and used as received. The characteristics of the solvents are reported in Table I.

TABLE I Characteristics of the solvents

Solvents	Boiling point (°C)	Density (kg/m^3)	Solubility in water (kg/100 kg)	Dielectric constant
Tetrahydrofuran (THF)	66.00	880	30.00	7.60
Chloroform ($CHCl_3$)	61.20	1500	0.80	4.81
Carbon tetrachloride (CCl_4)	76.70	1600	0.05	2.24

TABLE II Composition of the samples

Composite designation	Solvent	TEOS:H_2O (mole ratio)	Gelling time (days)	Gelling temperature (°C)	Appearance of the composites
ENR T	THF	1:2	5	25	Transparent
ENR CH	$CHCl_3$	1:2	5	25	Partly phase separated
ENR CC	CCl_4	1:2	7	25	Partly phase separated
ENR W1	THF	1:1	5	25	Transparent
ENR W2	THF	1:2	5	25	Transparent
ENR W4	THF	1:4	7	25	Partially opaque
ENR W6	THF	1:6	8	25	Opaque
ENR W8	THF	1:8	10	25	Opaque
ENR W10	THF	1:10	10	25	Opaque
ENR 50T	THF	1:2	2 + 3	50	Opaque
ENR 100T	THF	1:2	2 + 3	100	Opaque

2.2. Preparation of the hybrid composites

Epoxidised natural rubber (ENR) was dissolved in the solvents ($THF/CHCl_3/CCl_4$) by maintaining a constant rubber to solvent ratio at 1:3 (w/v). Tetraethoxysilane (TEOS) and water in the molar proportions of 1:2 [11] with 45 wt% of TEOS with respect to the rubber, was added to the solvated rubber under stirring conditions at room temperature. The pH of the reaction medium was maintained at 1.5 by adding appropriate amount of concentrated HCl. The mixture was stirred for 30 min at room temperature for homogenization. The resultant solution was cast over plane glass plate for gelation at room temperature till they showed no weight variation. The designation of the samples and their respective gelling time are reported in Table II.

Variation in the proportions of TEOS to water mole ratio in the hybrid composites was carried out by dissolving the rubber in THF at a constant pH of 1.5. The amount of TEOS was kept fixed to 45 wt% with respect to the rubber. The variation in the molar proportion of water and the gelling time of the respective samples are reported in Table II. Appearance of the samples varied from transparent to nearly opaque (Table II). Addition of curatives for the rubber phase within the composites was performed by adding DCP (0.75 phr) to the rubber solution at room temperature after initial stirring for 30 min with TEOS, HCl and water. After thorough mixing for another 30 min, the resultant solution was cast on plane glass plate for gelation under controlled conditions for 5 days at room temperature. The resultant films were then subjected to curing reaction in an oven at 160°C for 30 min [11]. The crosslinked hybrid composites were opaque in appearance.

ENR, dissolved in THF, was mixed with TEOS and water in the molar proportions of 1:2 at room temperature, at identical pH, following the procedure mentioned earlier. The cast films were kept for 2 days at room temperature and then allowed to gel for another 3 days at 50 and 100°C, respectively in an oven. The initial gelation period of 2 days at room temperature was allowed to restrict the formation of pores over the samples by rapid evaporation of solvents and by-products of the hydrolysis and condensation of TEOS.

2.3. Characterization of the composite films

2.3.1. Infrared spectroscopy (FTIR)

The infrared spectra of the hybrid composite films were recorded with a Nicolet Nexus FTIR spectrophotometer in an ATR mode using 45° KRS5 prism at room temperature (25°C). The samples were scanned from 2000 to 700 cm^{-1} with a resolution of 4 cm^{-1}. All the spectra were taken after an average of 32 scans for each specimen.

2.3.2. Optical density (OD) and transmission loss

The infrared optical density of the uncured composites were taken as the infrared absorbance values (A) of the composite films of average thickness 0.25 mm, which was expressed as

$$\text{OD} = A = \log_{10}(I/I_0). \quad (1)$$

where I_o is the intensity of light incident on the sample and I is the reflected beam intensity. The higher was the optical density (OD), the lower was the transmittance.

Optical density times 10 was equal to the transmission loss which was expressed in decibel (dB) ($\text{dB} = 10\log_{10}(P_1/P_2)$, where P_1 and P_2 are the actual powers) [14].

2.3.3. Transmission electron microscopy (TEM)

Transmission electron microscopic studies were carried out using TEM (model C-12, Philips) on very thin films (100 nm) of uncured hybrid composites, cast directly over the copper grids of 300 mesh size. The acceleration voltage was 120 kV. The magnifications of the images are mentioned in the respective captions.

2.3.4. Scanning electron microscopy (SEM)

Scanning electron microscopic investigation of the uncured hybrid composites was made by using a Jeol JSM 5800 scanning electron microscope. The sample films were sputter coated with gold. The operating voltage was maintained at 20 kV and the magnification was 10000×.

2.3.5. Dynamic mechanical thermal analysis (DMTA)

Dynamic mechanical thermal analysis of the uncured hybrid composite films was done in a DMTA IV, RHEOMETRIC SCIENTIFIC under tension mode. The experiments were carried out at a frequency of 1 Hz. The measurements were taken from −80 to 100°C at a heating rate of 2°C/min. The data were analyzed using RSI Orchestrator application software on an ACER computer attached to the machine. The storage modulus and loss tangent ($\tan\delta$) were measured for all the samples under identical conditions.

2.3.6. Mechanical property studies

The mechanical properties of the cured and the uncured composite films were recorded in a universal testing machine (UTM, Zwick 1445) with tensile specimens, punched out from the cast films using ASTM Die C. The tests were carried out as per ASTM D 412-99 method at 25 ± 2°C at a cross head speed of 500 mm/min. The average value of three tests was reported for each sample.

2.3.7. Swelling behavior of the composite films

Equilibrium swelling of the uncured hybrid composite films was determined in THF, under ambient conditions after 72 h, by measuring the equilibrium weights. The equilibrium swelling index (α) was calculated by using the following formula:

$$\alpha = ((W_\text{f} - W_\text{i})/W_\text{i}) \times 100 \quad (2)$$

where W_f is the final weight and W_i is the initial weight.

2.3.8. Measurement of ash content

Ash content of the uncured hybrid composites was determined by heating the samples in a muffle furnace at 800°C for 8 h. The difference between the initial and the final weights was recorded and the data were expressed as wt% ash content of the composites.

3. Results and discussion

3.1. Infrared spectroscopic analysis (FTIR) and solubility studies

Fig. 1a exhibits the Fourier Transform infrared spectrograph of the uncured ENR/silica hybrid composites, prepared by using different solvents. The IR spectra of pure ENR film, cast directly from THF, is also given in the same figure for comparison. The characteristic absorptions of the samples are registered in Table III. Absorptions at 1446 and 1380 cm^{-1} due to the C—H bending and deformation vibrations of the hydrocarbon backbone and absorptions due to olefinic unsaturations in the rubber at 1650 cm^{-1}, appear in the spectrum of the pure ENR. C—O symmetric stretching for the epoxy group in the rubber is indicated by the wide absorptions in the region of 1100–1000 cm^{-1}, while C—O

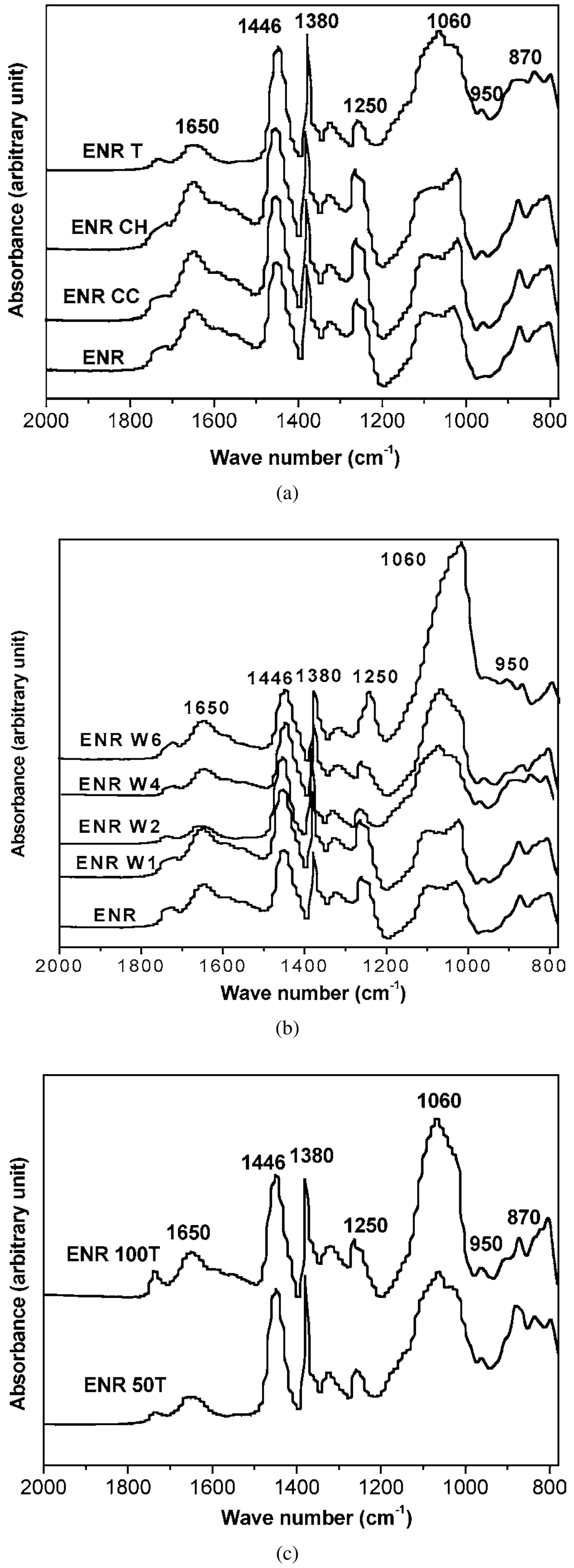

Figure 1 (a) FTIR spectrograph of the uncured ENR/silica hybrid composites prepared by using different solvents. (b) FTIR spectrograph of the representative uncured ENR/silica hybrid composites prepared by using different TEOS to water mole ratio. (c) FTIR spectrograph of the uncured ENR/silica hybrid composites prepared with different gelation temperature.

TABLE III Characteristic infrared absorption peaks for the uncured ENR/silica organic-inorganic hybrid composites

Peak absorption values (cm^{-1})	Peak designation
1650	C═C stretching
1446	C—H bending
1380	C—H deformation
1250	C—O asymmetric stretching
1100–1000	(symmetric) C—O and Si—O—Si stretching
950	Si—O stretching for silanol
870	C—O—C epoxy ring vibration

TABLE IV Ash content data for the representative uncured hybrid composites

Composite designation	Ash (wt%)
ENR T	16.5
ENR CH	9.5
ENR W1	11.0
ENR W4	17.0
ENR W6	18.5
ENR 100T	16.0

asymmetric stretching occurs at 1250 cm^{-1} (Fig. 1a). Absorptions at around 870 cm^{-1} denote the epoxy ring (C—O—C) vibrations in the rubber. Strong absorptions due to Si—O—Si stretches for the silica particles, formed in-situ in the hybrid composites, is likely to overlap with the wide absorptions within the range of 1100–1000 cm^{-1} of the pure rubber sample (Fig. 1a). ENR CC and ENR CH exhibit almost similar absorption intensity to that of the pure rubber, within this region (1100–1000 cm^{-1}) which reveals very small amount of silica generation within the respective hybrids. ENR T shows the maximum absorbance within that region and therefore indicates the highest silica concentration in the ENR T hybrid composite. It is further supported by the ash content data of the respective samples as registered in Table IV. Weak absorptions due to the Si—O stretches for the silanol groups (Si—OH) appear around 950 cm^{-1} for ENR CH and ENR CC. In ENR T, the same area becomes broad and the sharpness of the absorption peak at 870 cm^{-1} due to epoxy ring vibration is also reduced. Broad absorption in this region may be due to overlapping of the Si—O stretching of the silanol groups and the C—O—C ring vibrations. Decrease in sharpness of the peak at 870 cm^{-1} possibly indicates the reduction in the concentration of epoxy groups in the hybrid, due to probable chemical interaction occurring with the silanol moieties, as shown by Scheme 2. Solubility studies of the hybrid composites in THF under ambient condition, show the formation of the gel after 72 h, supporting the above statement.

Generation of lower amount of silica in ENR CH and ENR CC compared to ENR T may be explained by considering the nature of the respective solvents. Both $CHCl_3$ and CCl_4, have low polarity (low dielectric constant values) and poor water miscibility (Table I). Poor water affinity of $CHCl_3$ and CCl_4 compared to THF is a key factor, because it produces inhomogenity in the system as ENR CH and ENR CC show partial phase separation, which may be due to improper dispersion of the silanol groups on account of low polarity of $CHCl_3$ and CCl_4 (Fig. 1a).

Fig. 1b displays the FTIR spectra of the representative uncured ENR/silica hybrid composite films,

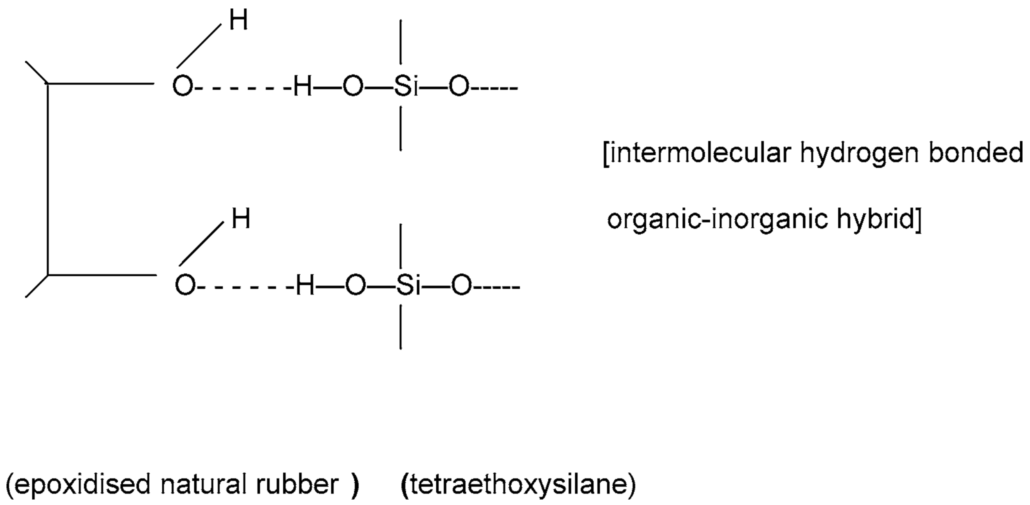

Scheme 2

prepared in THF by using different TEOS to water ratios. ENR W1 is almost the replica of the pure ENR sample, as it shows very little silica formation (evident from low Si—O—Si stretching around 1100–1000 cm^{-1}, Fig. 1b). It is probably due to lower extent of hydrolytic reaction of TEOS on account of lower proportion of water compared to the stoichiometric requirement. ENR W2, ENR W4 and ENR W6 display progressive increase in absorption intensity in the same region. The corresponding epoxy ring vibrations at 870 cm^{-1} gradually become wider and probably overlap with the silanol stretches, with the addition of higher proportions of water (Fig. 1b). It may be due to higher extent of hydrolysis in TEOS, favored by the addition of comparatively higher amount of water. This would generate more silanol groups which interact with the di-ol moieties of the rubber (Scheme 2). Solubility (α) studies of the respective composites in THF under ambient conditions for 72 h, provides ample support to this opinion, as it gives marginally higher proportion of gel formation with the increase in proportion of water in the hybrid composites ($\alpha = 357\%$ for ENRW2 and 327% for ENRW6). The ash content data for ENRW2 and ENRW6 in Table IV are also in line with the result. Generation of excess silanol groups may have enhanced the polycondensation reaction and results in local agglomeration of silica particles. ENR W4 gives partial phase separation and the opacity further increases for ENR W6. ENR W8 and ENR W10 are completely opaque in appearance on account of more agglomerated forms of silica within the composites. Therefore, increase in absorption intensity due to the presence of silica particles (1100–1000 cm^{-1}) in the composites (ENR W4 and ENR W6, Fig. 1b), may be due to the agglomerated silica structures in the respective composites.

Fig. 1c exhibits FTIR spectra for the uncured ENR/silica hybrid composites prepared from THF by varying the temperature of condensation. Absorption due to Si—O—Si stretching (1100–1000 cm^{-1}) is higher for ENR 100T compared to ENR 50T. It may be due to the effect of local agglomeration of silica particles on account of the enhanced rate of the reaction at elevated temperature in ENR 100T. Absorbance due to the silanol (950 cm^{-1}) and the epoxy groups (870 cm^{-1}) are comparable for both ENR 50T and ENR 100T though the epoxy ring vibration at 870 cm^{-1} is prominent for ENR 50T and ENR 100T compared to ENR T (Fig. 1a, TEOS: water in mole ratio of 1:2 but gelled at room temperature). It may be due to the effect of agglomeration of silica that cause lower interaction with the rubber phase in the respective composites (ENR 50T and ENR 100T are not transparent in appearance).

The infrared optical density values (OD) for the representative hybrid composites are registered in Table V. A significant higher OD value for ENR CH is noticed compared to ENR which indicates more opacity in the infrared region for the former. Similarly, ENR W4 and ENR 100T also exhibit relatively lower clarity compared to pure ENR (the OD values are high), while ENR W2 shows an OD value close to ENR. The higher OD values compared to pure ENR cause more transmission loss of the infrared light (Table V) within the respective composites. The possible explanation may be the phase separated morphology at the organic-inorganic interfaces of the hybrid composites that reduces the infrared transparency. These are discussed below.

3.2. Morphological investigation

Fig. 2a–b displays the representative TEM micrographs of the uncured ENR T and the ENR CH hybrid composites. Micrograph for ENR T shows the existence of black spherical silica particles dispersed over the rubber matrix. The average dimension of the particles is around 90 nm. The picture discloses few areas where local agglomeration has taken place. It probably indicates the limitations of the loading of TEOS in the

TABLE V Infrared optical density and the transmission loss values for the representative uncured hybrid composites

Sample	Optical density	Transmission loss (dB)
ENR	0.15	1.5
ENR CH	0.22	2.2
ENR W2/ENR T	0.17	1.7
ENR W4	0.25	2.5
ENR 100T	0.26	2.6

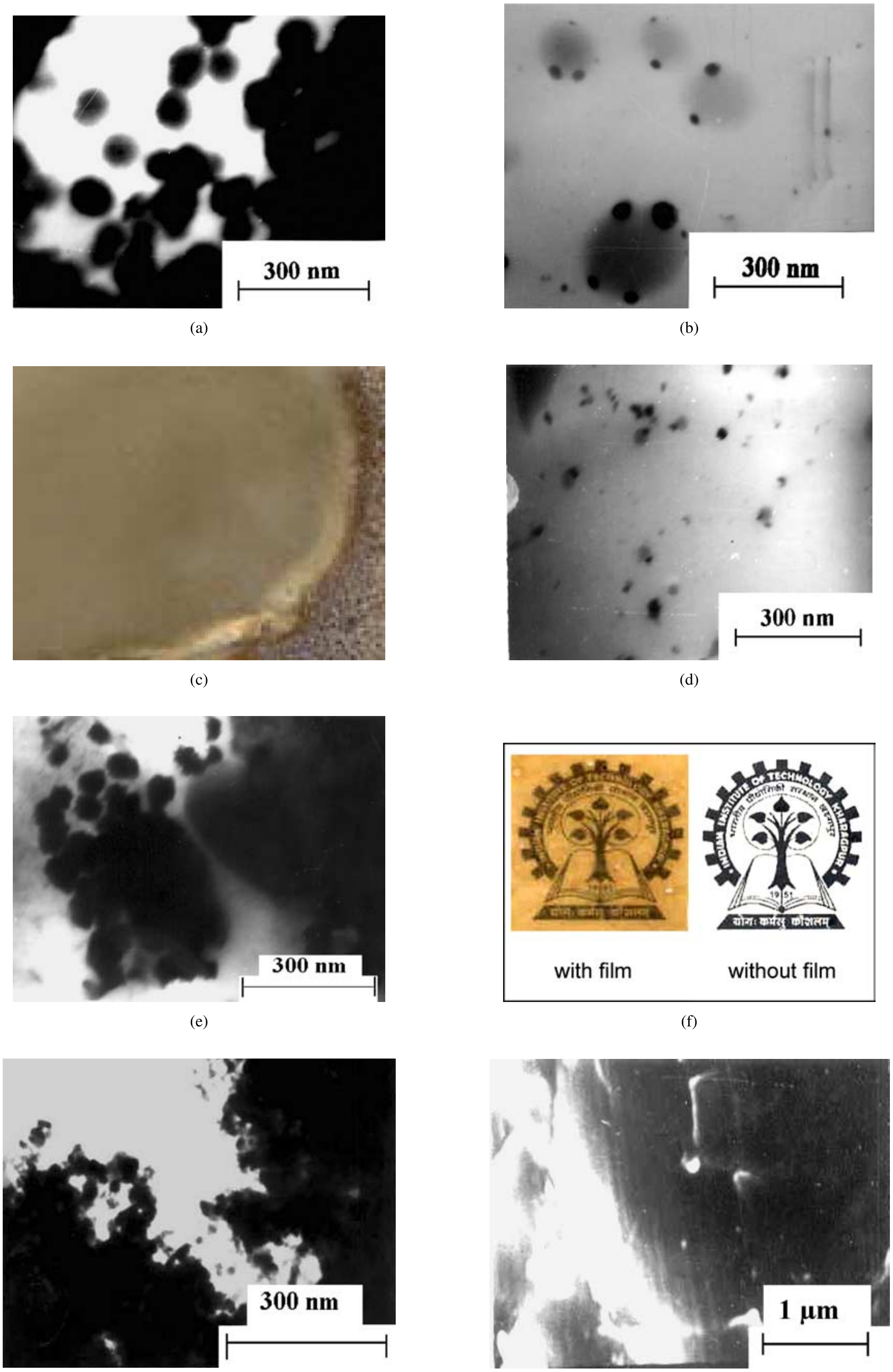

(a) (b) (c) (d) (e) (f) (g) (h)

Figure 2 Photographs of the representative uncured hybrid composites. (a) TEM micrograph of ENR T (80000×) (b) TEM micrograph of ENR CH (80000×) (c) Visual appearance of ENR CH (d) TEM micrograph of ENR W1(80000×) (e) TEM micrograph of ENR W4 (80000×) (f) Visual appearance of ENR W4 over a logo shown beside (g) TEM micrograph of ENR W6 (80000×) and (h) SEM micrograph of ENR 100T (10000×).

rubber that may lead to phase separation at the interfaces by the large scale agglomeration of silica particles. ENR CH displays the presence of very few silica particles, scattered over the rubber matrix (Fig. 2b). The average dimension of the silica particles in ENR CH is close to 25 nm. The smaller size of the silica particles is probably due to the poor condensation of silanol groups, as already discussed in the earlier section. Phase separation within the composite is evident from the appearance of the film (average thickness 0.25 mm), displayed in Fig. 2c. Fig. 2d–e shows the TEM photographs of the representative uncured ENR/silica hybrids prepared by using different TEOS to water ratio. ENR W1 displays very small sized spherical silica particles of average dimension of 25 nm (Fig. 2d). The small size of the silica particles is probably due to the inadequate hydrolysis of TEOS, as the proportion of water is well below the stoichiometric requirement. ENR W4 in Fig. 2e gives comparatively bigger size silica particles (average dimension 90 nm) along with some agglomerated silica phase, probably due to greater extent of hydrolysis and condensation reaction compared to ENR W1 (Fig. 2d). Appearance of ENR W4 hybrid composite film is displayed in Fig. 2f. The film partially loses its optical clarity on account of the local agglomeration of silica particles. TEM micrograph of ENR W6 exhibits silica clusters that fall in the micrometer range (2 μm, Fig. 2g). Accelerated condensation in ENR W6 on account of high concentration of silanol groups may lead to the enhanced coalescence of the silica particles. The composite (ENR W6) is almost opaque in appearance as the phase separated silica particles scatter light. Fig. 2h exhibits the SEM image of ENR 100T. The figure displays the phase separated morphology of the composite. Application of heat accelerates the condensation reaction by rapidly removing water from the system thereby inducing the formation of silica clusters.

3.3. Dynamic mechanical thermal analysis

Fig. 3 shows the representative storage modulus and loss tangent curves for the uncured ENR/silica hybrid composites, studied within the temperature range of −80 to 100°C. The storage modulus value explains the elastic nature, whereas, loss tangent symbolizes the viscous loss characteristics of the hybrids. Table VI depicts the storage modulus values of the uncured composites taken at three different temperatures arbitrarily chosen at −50°C, T_g and 50°C. Hybrid composites from ENRT show the highest modulus values compared to ENR CH and ENR CC at all the three temperatures (Fig. 3a and Table VI). ENR CH displays marginally higher values than those of ENR CC. Polymer-filler interaction through largest number of silica particles in ENR T may cause best mechanical reinforcement within the composite. Fig. 3b displays the storage modulus values for the uncured ENR/silica composites prepared by varying the TEOS to water mole ratio in THF. ENR W2 and ENRW4 show the highest modulus at all the three temperatures compared to the other composites although the difference in modulus values for the samples is not large as evident from Fig. 3b and Table VI. Among the hybrid composites prepared by using different condensation temperatures, ENR T and ENR 50T display almost similar modulus values while the respective modulus values for ENR 100T are marginally lower (Fig. 3c and Table VI). As stated earlier, accelerated condensation at high temperature (100°C), probably induces silica agglomeration within the hybrid composites and therefore ENR 100T shows lower modulus values.

A comparative study on the loss tangent peak height values at T_g gives an idea about the extent of restricted polymer chain movements within the hybrid composites during the glass-rubber transitions. More is the polymer-filler interaction, lower would be the tan δ peak height (tan δ_{max}). Table VI displays the tan δ_{max} of the uncured ENR/silica hybrid composites. A drop in the peak height value is noticed from ENR CC to ENR CH hybrid composites, while tan δ_{max} decreases sharply for ENR T. The T_g values of the respective composites are given in Table VI. Higher T_g value for ENR T with respect to the other composites implies better polymer-silica interactions in ENR T. There is a marginal decrease in tan δ_{max} from ENR W1 to ENR W2 (Fig. 3b and Table VI). This is probably due to the conjugative effect of higher silica generation and nanolevel dispersion in ENR W2 compared to ENR W1. The same value is found to increase from ENR W2 (and ENR W4) to ENR W6. It may be due to the formation of silica aggregates within the respective composites as the hydrolysis of TEOS is accelerated by the addition of higher proportion of water. The T_g value for the composites (ENRW1, W2, W4 and W6) follows the reverse trend (Table VI). Gradual increase in tan δ_{max} from the composite prepared at ambient conditions to those at 50 and 100°C, may be due to the formation of silica aggregates within the system, that offer lesser surface area for interaction with the polymer chains (Fig. 3c and Table VI).

TABLE VI Dynamic mechanical properties for the uncured hybrid composites

Composite designation	Log E' (Pa) −50°C	Log E' (Pa) T_g	Log E' (Pa) 50°C	Tan δ_{max}	T_g (°C)
ENR T	9.58	8.00	6.57	1.68	−13
ENR CH	9.50	7.78	6.24	1.80	−27
ENR CC	9.49	7.27	6.19	1.95	−29
ENR W1	9.53	8.01	6.48	1.71	−15
ENR W2	9.58	8.00	6.57	1.68	−13
ENR W4	9.57	8.06	6.57	1.68	−14
ENR W6	9.50	7.98	6.43	1.75	−18
ENR 50T	9.55	7.99	6.51	1.70	−14
ENR 100T	9.53	7.96	6.49	1.72	−15

3.4. Mechanical properties

Fig. 4 displays the representative tensile stress-strain curves for the uncured ENR/silica hybrid composites. The curves show significant yielding after an elongation of 300% that resembles typical uncured elastomeric behavior. For all the uncured composites, discussed within this section, the tensile strength is taken as the maximum stress point in the stress-strain curves and the corresponding values are registered in Table VII.

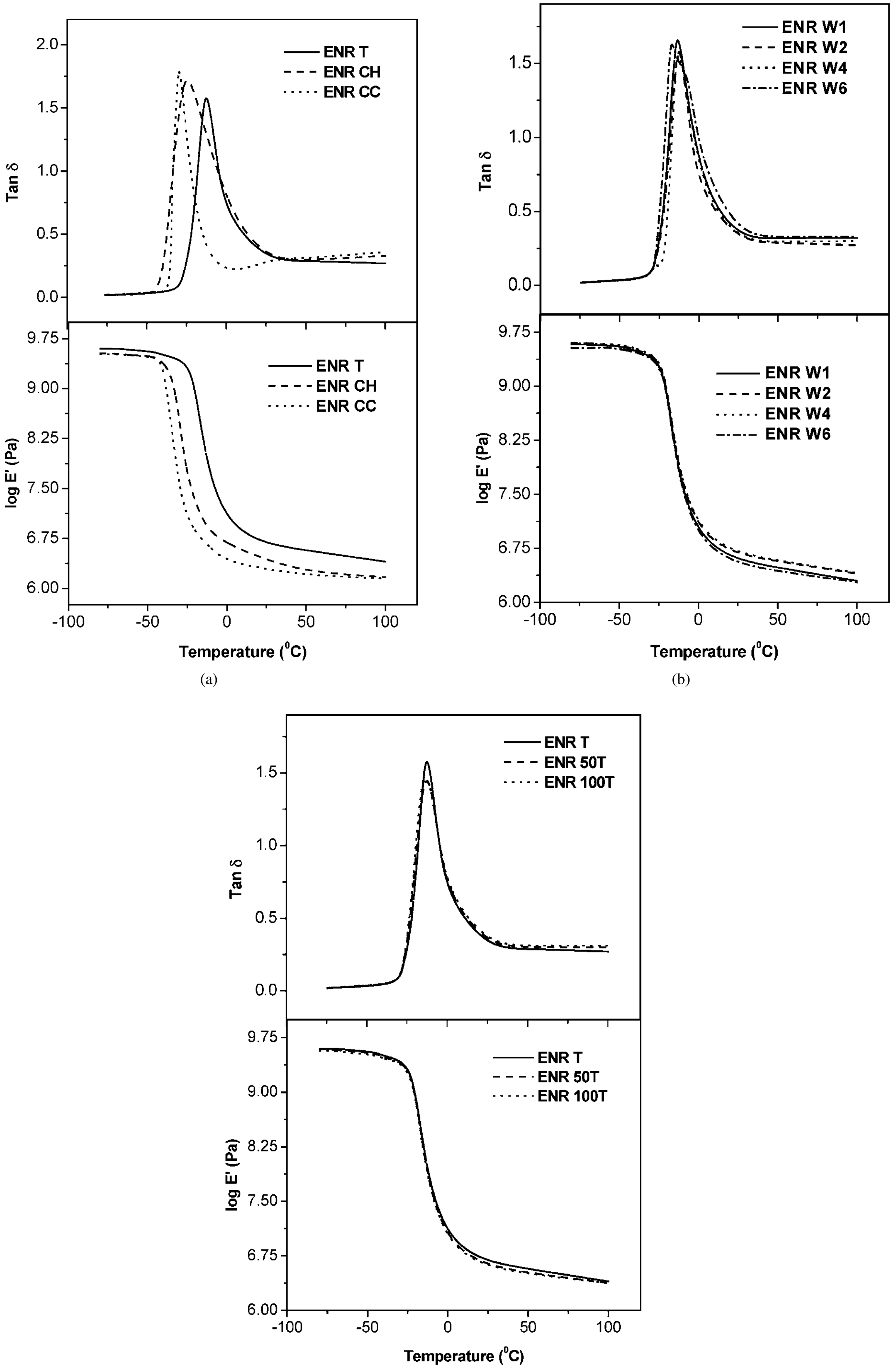

(a)

(b)

(c)

Figure 3 (a) Storage modulus (log scale) and tan δ curves for uncured ENR/silica hybrid composites prepared by using different solvents in the temperature range −80 to 100°C. (b) Storage modulus (log scale) and tan δ curves for the uncured ENR/silica hybrid composites prepared by using different TEOS to water mole ratio in the temperature range −80 to 100°C. (c) Storage modulus (log scale) and tan δ curves for the uncured ENR/silica hybrid composites prepared at different gelling temperature in the temperature range −80 to 100°C.

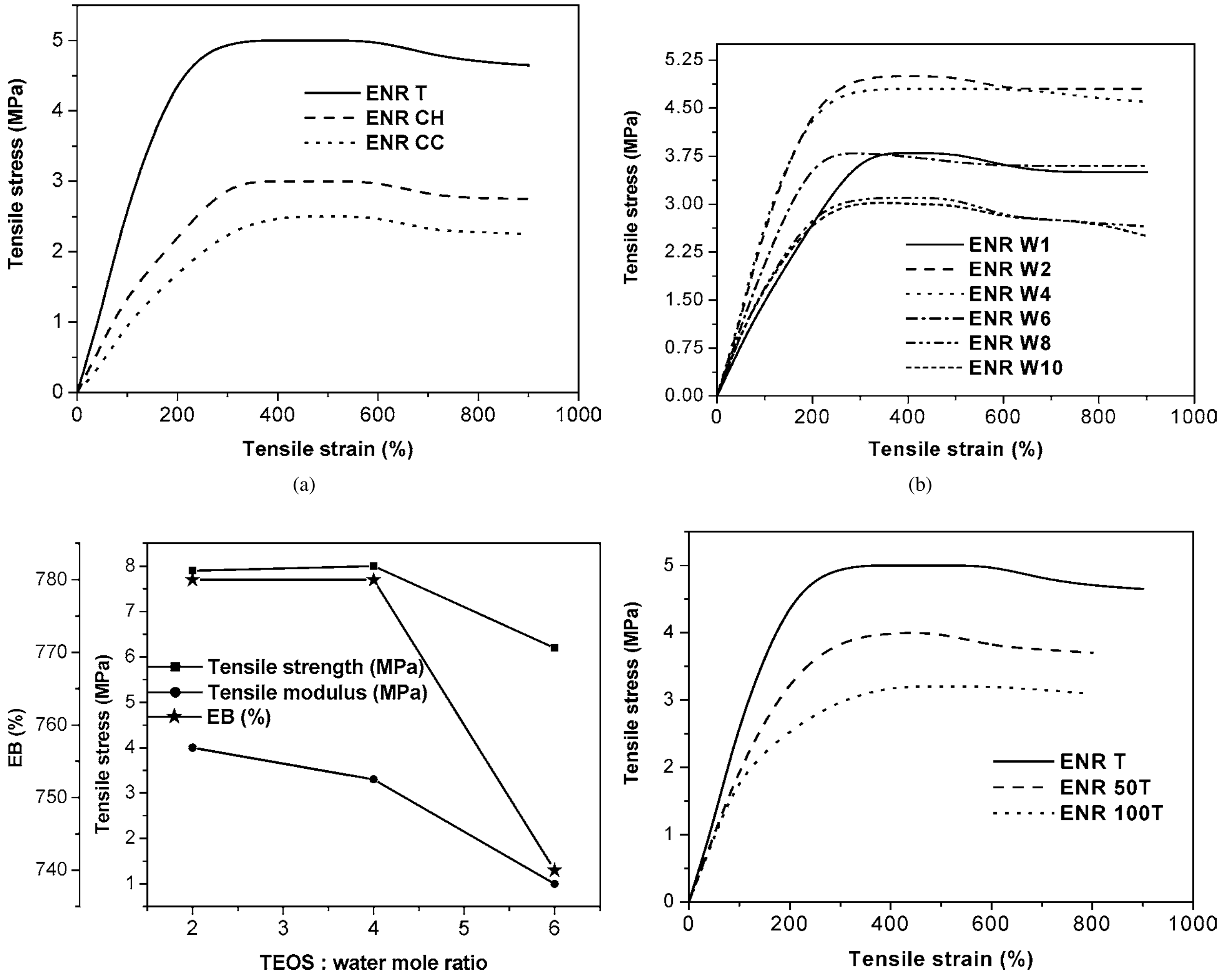

(a) (b)

(c) (d)

Figure 4 (a) Tensile stress-strain curves for the uncured ENR/silica hybrid composites prepared by using different solvents. (b) Tensile stress-strain plots for the uncured ENR/silica hybrid composites prepared by using different TEOS to water mole ratio. (c) Tensile strength, tensile modulus (100%) and elongation at break (%) values for the representative cured hybrid composites prepared by using different TEOS to water mole ratio. (d) Tensile stress-strain plots for the uncured hybrid composites prepared at different temperature for gelation.

Fig. 4a exhibits the tensile stress-strain curves for the uncured ENR/silica hybrid composites prepared in different solvents. ENR T registers higher tensile strength (67%) and 100% modulus (95%) compared to ENR CH, while the improvement is about 100 and 180% respectively from that of ENR CC (Table VII). The strength of the composites is a direct function of polymer-filler interaction which is maximum in ENR T as the polarity of THF has favored the in-situ silica generation. For $CHCl_3$ and CCl_4, lower silica concentration as well as poor polymer-silica interaction may produce an adverse effect on the strength of the composites.

TABLE VII Mechanical properties of the uncured ENR/silica hybrid composites

Composite designation	Tensile modulus at 100% elongation (MPa)	Tensile strength (MPa)	Elongation at break (%)
ENR T	2.70	5.00	>900
ENR CH	1.40	3.00	>900
ENR CC	1.00	2.50	>900
ENR W1	1.50	3.80	>900
ENR W2	2.70	5.00	>900
ENR W4	2.80	4.50	>900
ENR W6	2.10	3.80	>900
ENR W8	1.72	3.10	>900
ENR W10	1.70	3.05	>900
ENR 50T	2.00	4.00	800
ENR 100T	1.89	3.20	780

Fig. 4b shows the tensile stress-strain curves for the uncured hybrid composites, prepared in THF by using different TEOS to water mole ratio. ENR W2 and ENR W4 show comparable tensile strength and modulus values which are higher than the values exhibited by ENR W1 and ENR W6-10 hybrid composites. ENR W1 shows very low concentration of silica (Fig. 2d) while for ENR W6-10, the silica agglomerations are dominant. Both these phenomena have resulted in poor polymer-filler interaction that may have acted in favor of strength deterioration in the respective composites compared to ENR W2 and ENR W4. The phase separated texture of the films (Table II) with higher proportion of water (proportion of water higher than 4% with respect to TEOS) also supports this observation.

Fig. 4c exhibits the tensile strength and tensile modulus values (100%) for the representative DCP crosslinked composites ENR W2, ENR W4 and ENR W6. ENR W2 and ENR W4 exhibit higher tensile strength and modulus (almost 60 and 20% respectively) than those of the uncured composites. It may be due to the synergism between the crosslinked rubber phase and the nanosilica dispersion [9]. ENR W6 contains more of agglomerated silica structures compared to ENR W2 and ENR W4. Low interfacial interaction due to broad size distribution of silica particles may be responsible for comparatively lower improvement in tensile strength and modulus values (50 and 10% respectively) for ENR W6. The elongation at beak values for the cured composites decrease from ENR W2 to ENR W6 which may be due to the existence of bigger sized silica particles that act as flaw in the system and cause sample failure.

Fig. 4d displays the tensile stress-strain curves for the uncured hybrid composites, prepared by varying the condensation temperature of the hybrids. At high temperature (higher than the ambient) generation of agglomerated silica structures due to accelerated condensation becomes more probable, which decrease the tensile strength and modulus values by providing less surface area for interaction with the polymer chains (evident from lower tensile strength and modulus values of ENR 50T and ENR 100T compared to ENR T in Table VII).

4. Conclusions

Structure-property relationship of the ENR/silica organic-inorganic hybrid composites prepared by varying the nature of solvents, TEOS to water mole ratio and temperature at fixed concentration of TEOS (45 wt%) and constant pH of the reaction medium has been studied here. Nanolevel dispersion of silica particles is obtained in the composite prepared in THF by using 1:2 TEOS to water mole ratio under room temperature conditions. The solvents $CHCl_3$ and CCl_4 do not give effective condensation of silanol groups probably due to lower polarity and poor water miscibility. On increasing the molar proportion of water beyond 4, the resultant composites display phase separation to a greater extent which causes agglomeration of silica particles, evident from the morphological studies. Infrared spectroscopic data apparently indicate high silica concentration in the composites gelled at high temperature (higher than the ambient temperature) as well as in those have higher proportion of water in the TEOS/water mixture. Infrared optical density as well as the transmission loss are increased for the hybrid composite prepared by using nonpolar solvents, high TEOS to water mole ratio (higher than 1:2) and high gelation temperature. Dynamic mechanical analysis exhibits comparatively higher storage modulus and lower tan $\delta_{\max}$ for the nanocomposites (ENR W2 or ENR T and ENR W4) than the other composites (ENR CH, ENR CC and ENR W6). Comparatively higher tensile strength and modulus values (100% elongation) are obtained with the nanocomposite ENR W2 (or ENR T). ENR CH, ENR CC and ENR W1 show inferior mechanical strength due to the lack of silica generation in the systems. ENR CH and ENR CC do not favor dispersion and condensation of silanol moieties while ENR W1 do not give effective condensation reaction probably due to lower extent of hydrolysis reaction in TEOS on account of very low water concentration compared to the stoichiometric requirements. The composites ENR W6-W10 and also ENR 50T and ENR 100T, exhibit low mechanical strength, which may be due to the poor interfacial interaction between the polymer matrix and the silica, as the filler is present in more aggregated structures. The ENR W2, W4 and W6 composites show the similar trend after crosslinking of the rubber phase using DCP. The elongation at break values for the composites studied here are generally very high (700 to 900%).

References

1. R. M. LAINE, C. SANCHEZ, C. J. BRINKER and E. GIANNELIS in "Organic/Inorganic Hybrid Materials" (Materials Research Society, 2000) Vol. 628.
2. C. SANCHEZ and B. LEBEAN, *MRS Bull.* **26** (2001) 377.
3. T. OGOSHI, H. ITOH, K. M. KIM and Y. CHUJO, *Macromolecules* **35** (2002) 334.
4. C. J. BRINKER and G. W. SCHERER, in "Sol-Gel Science: The Physics and Chemistry of Sol-Gel Processing" (Academic Press Inc, California, USA, 1990).
5. G. L. WILKIS, H.-H. HUANG and R. H. GLASER, *Polym. Prepr.* (1990) 207.
6. S. SADHU and A. K. BHOWMICK, *Rubber Chem. Technol.* **76** (2003) 860.
7. *Idem.*, *J. Appl. Polym. Sci.* **92** (2004) 698.
8. *Idem.*, *J. Polym. Sci. Part B: Polym. Phys.* **42** (2004) 1573.
9. A. BANDYOPADHYAY, A. K. BHOWMICK and M. DE SARKAR, *J. Appl. Polym. Sci.* **93** (2004) 2579.
10. A. BANDYOPADHYAY, M. DE SARKAR and A. K. BHOWMICK, communicated (2003).
11. *Idem.*, *Rubber Chem. Technol.* 2004 (Sept/Oct.)
12. J. JONAS, in "Science of Ceramic Chemical Processing" (Wiley, New York, 1986).
13. G. ORCEL and L.L. HENCH, *J. Non-Cryst. Solids* **79** (1986) 177.
14. www.its.bldrdoc.gov dated 01.03.04.

Received 24 March
and accepted 23 June 2004